CFD/CAA Analysis for a Wing Leading Edge Test in the Quiet Flow Facility
(Work in Progress)

Jeffrey Housman and Cetin Kiris
NASA Ames Research Center
Dogus Akaydin and Shayan Moini-Yekta
Science and Technology Corporation
Florence Hutcheson and Christopher Bahr
NASA Langley Research Center

Funded by the NASA Fundamental Aeronautics Program
Environmentally Responsible Aviation (ERA) Project

Spring 2015 Acoustics Technical Working Group Meeting
NASA Langley Research Center, April 21-22, 2015

Outline

- Objective and Approach
- Launch Ascent and Vehicle Aerodynamics (LAVA) Framework
- 3rd AIAA BANC Workshop: Slat Cove Noise
- Aerodynamic Characterization of Slat Configuration
- Summary

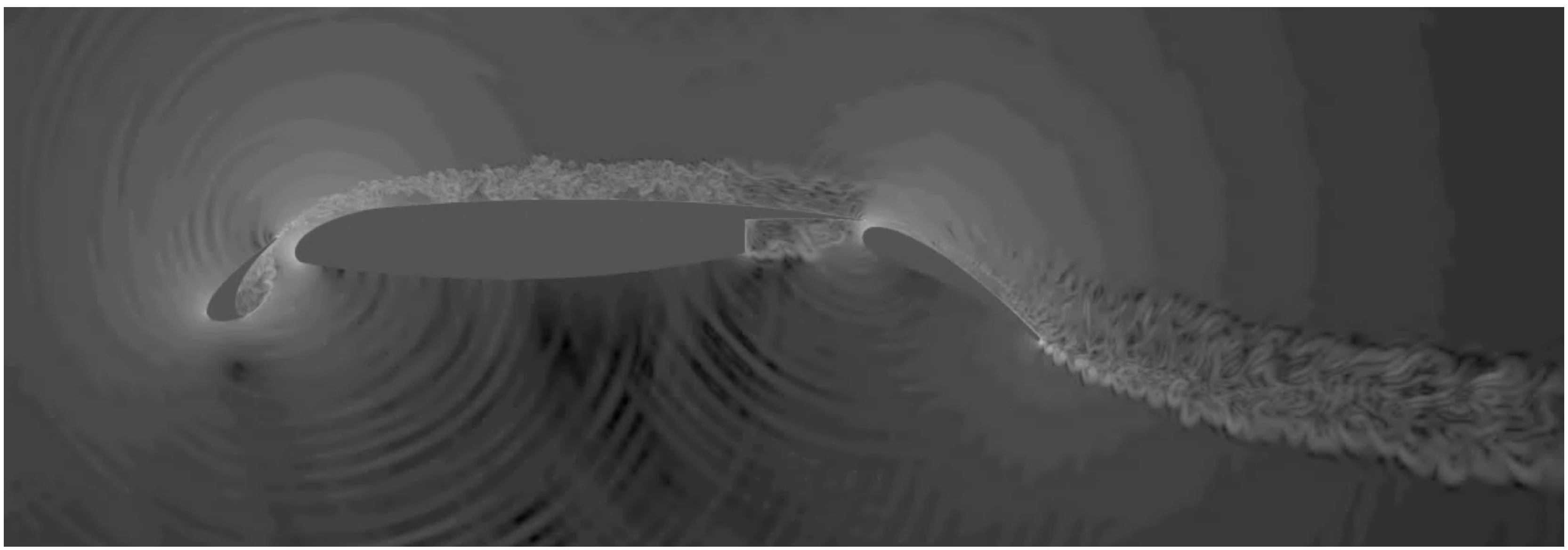

Outline

- Objective and Approach
- Launch Ascent and Vehicle Aerodynamics (LAVA) Framework
- 3rd AIAA BANC Workshop: Slat Cove Noise
- Aerodynamic Characterization of Slat Configuration
- Summary

Objective and Approach

Objective

- Compare noise source generation mechanisms between the conventional slat and LE Krueger flap high lift devices

Approach

- Aerodynamic characterization of a conventional slat configuration
- Design a LE Krueger flap with "equivalent aerodynamic performance"
- Identify noise generation mechanisms and compare far-field noise characteristics between the conventional slat and LE Krueger flap using both experimental and CFD/CAA analysis tools

Outline

- Objective and Approach
- **Launch Ascent and Vehicle Aerodynamics (LAVA) Framework**
- 3rd AIAA BANC Workshop: Slat Cove Noise
- Aerodynamic Characterization of Slat Configuration
- Summary

LAVA Framework

*Launch Ascent and Vehicle Aerodynamics Framework**

- Computational Fluid Dynamics (CFD) Solvers
  - Cartesian, Curvilinear, and Unstructured Grid Types
  - Overset Grid and Immersed Boundary Methods
  - Reynolds Averaged Navier-Stokes and hybrid RANS/LES Simulation Capabilities
- Computational Aeroacoustics (CAA) Solvers
  - Linear Helmholtz and Ffowcs Williams-Hawkings Formulations in the Frequency Domain
  - Radiating and Scattering Capabilities (linear Helmholtz)

Development Team


Cetin Kiris


Jeffrey Housman


Michael Barad

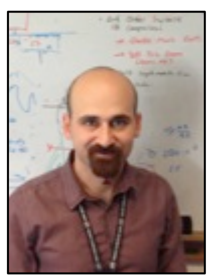
Emre Sozer


Christoph Brehm

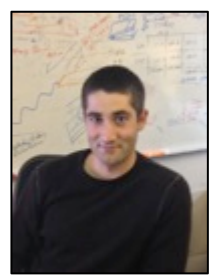
Shayan Moini-Yekta

*Kiris et. al. AIAA-2014-0070

LAVA Framework

Computational Approach

- 3-D Structured Overset Curvilinear Navier-Stokes Solver
- Spalart-Allmaras Turbulence Model
  - Unsteady DDES for acoustics (BANC-III)
  - Steady RANS for aerodynamics (QFF)
- Convective Flux Discretization
  - 4th – order central with 5th order WENO based matrix dissipation (BANC-III)
  - 6th – order HWCNS with high-order metrics (QFF)
- 2nd – order central differencing for viscous fluxes and time
- Implicit dual-time stepping (BANC-III)
  - 2 orders of magnitude residual drop (11 to 16 subs)
- Implicit Euler (QFF)
  - 3-4 orders of residual drop and steady force convergence

Outline

- Objective and Approach
- Launch Ascent and Vehicle Aerodynamics (LAVA) Framework
- **3rd AIAA BANC Workshop: Slat Cove Noise**
- Aerodynamic Characterization of Slat Configuration
- Summary

3^{rd} AIAA BANC Workshop: Slat Cove Noise

Geometric Model

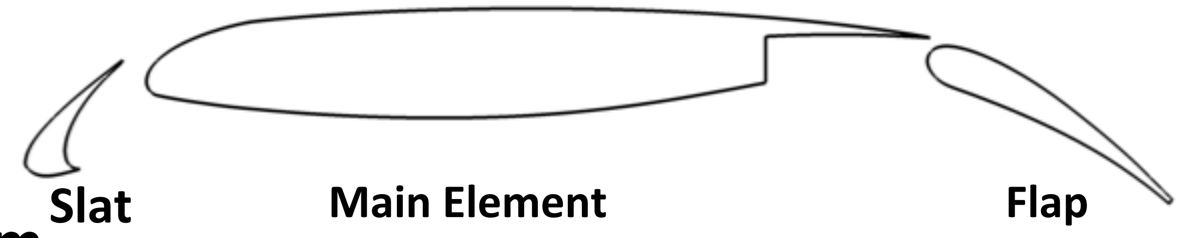

30P30N ConfigurationF

- **Stowed Chord c = 0.457 m**
  - **Slat Chord c_s= 0.15 c**
  - **Flap Chord = 0.3 c**
- **Model Span b = 1.016 m**
- **Simulated Span b_{sim} = 0.0508 m**
- **Periodic in Spanwise Direction**

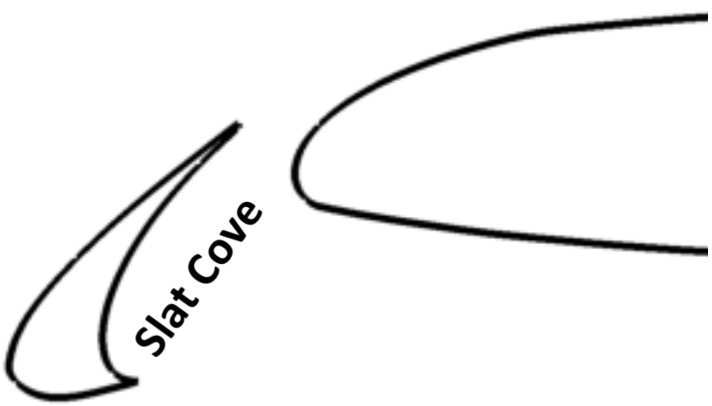

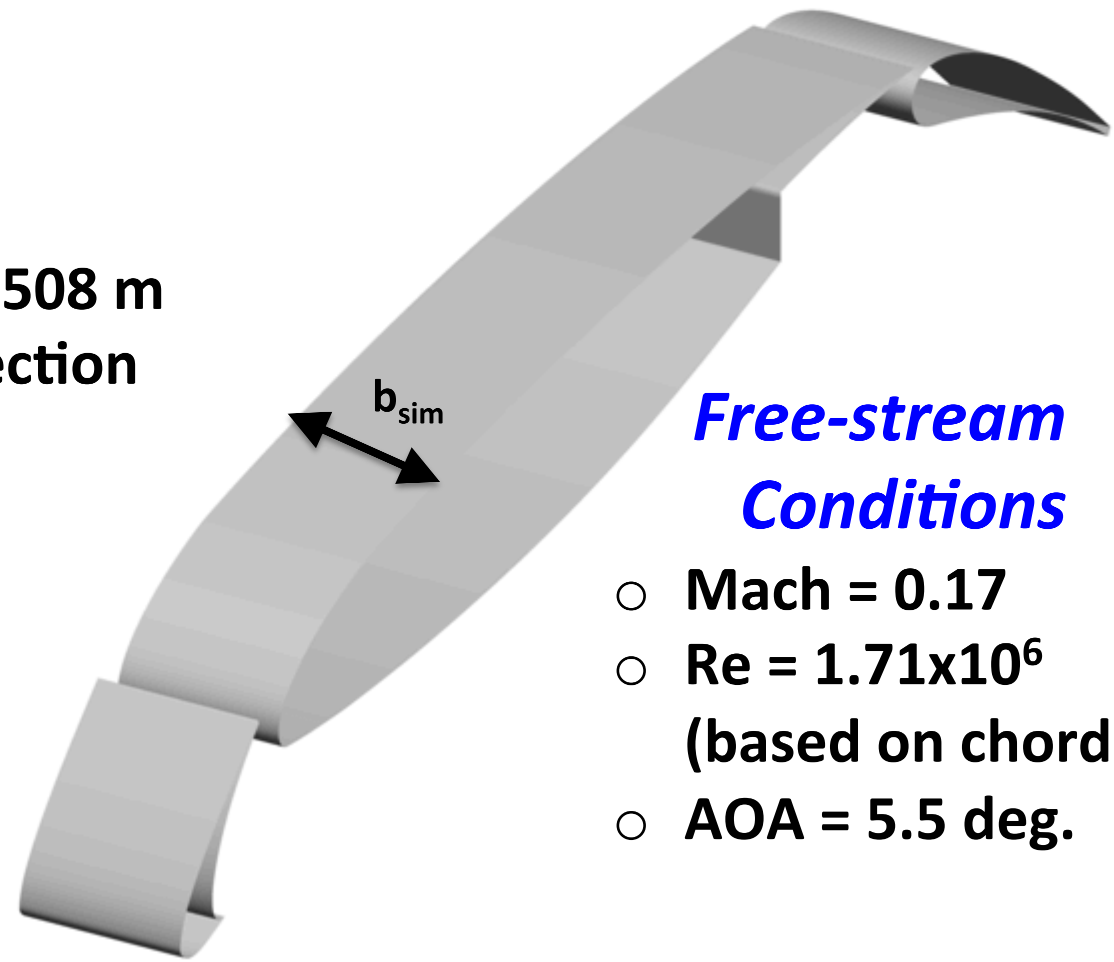

Free-stream Conditions

- **Mach = 0.17**
- **Re = 1.71×10^6 (based on chord)**
- **AOA = 5.5 deg.**

3rd AIAA BANC Workshop: Slat Cove Noise

- Goal was to assess the current capabilities of LAVA CFD/CAA tools applied to slat noise generation
- Flow physics is highly complex pushing the limits of current turbulence modeling and numerical methods

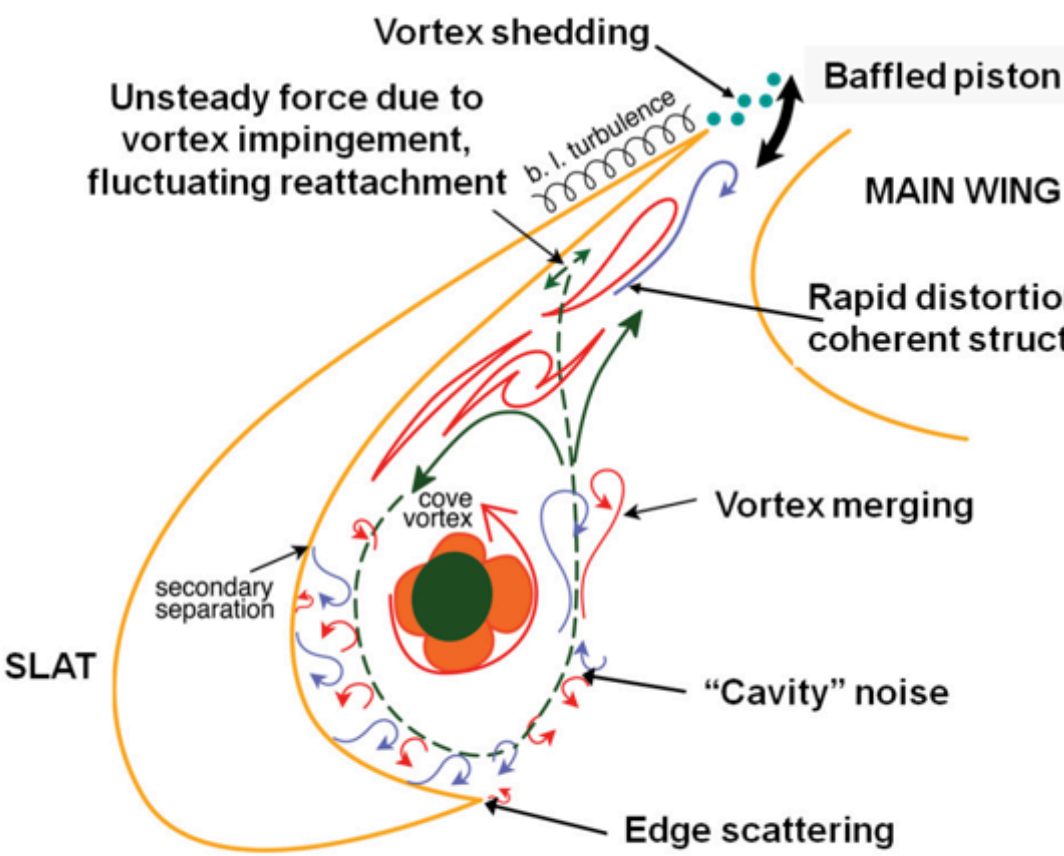

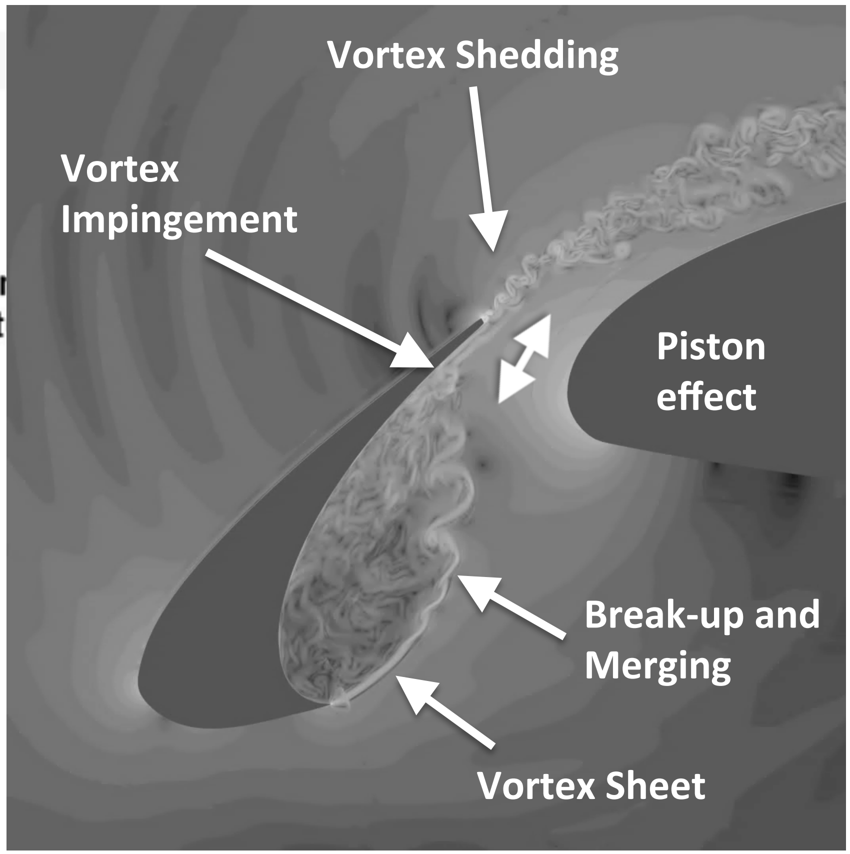

3rd AIAA BANC Workshop: Slat Cove Noise

Fine Mesh Overset Grid System for DDES Simulation

- 55 zones, 189.9 million grid points
- Span resolution ranges from 0.25 to 1.9 mm
- Grid aligned to streamwise flow features

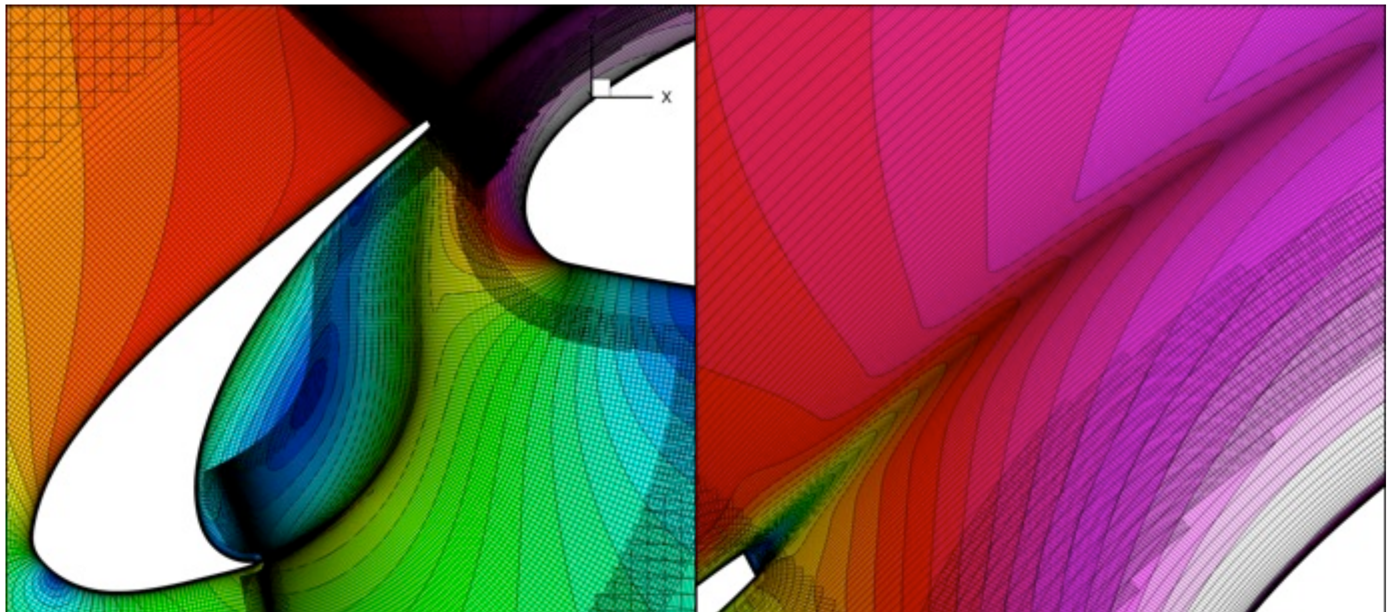

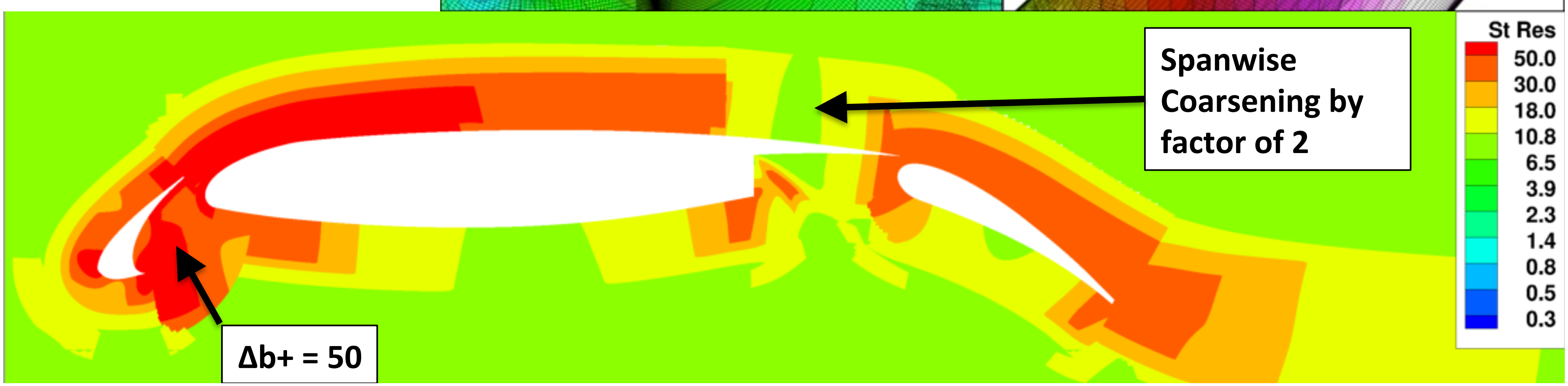

3rd AIAA BANC Workshop: Slat Cove Noise

Near-Field PSD

- Broadband noise characteristics within the slat cove are well captured for St < 10
- High frequency noise generated from the finite thickness TE of the slat is observed at St ≈ 28

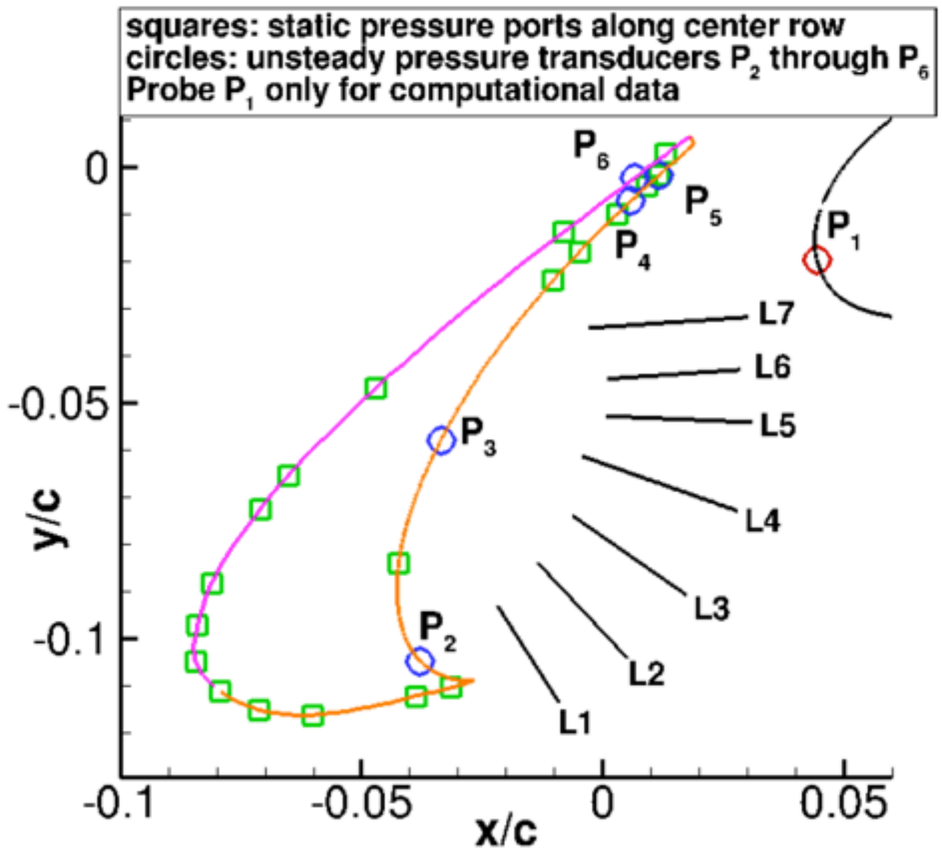

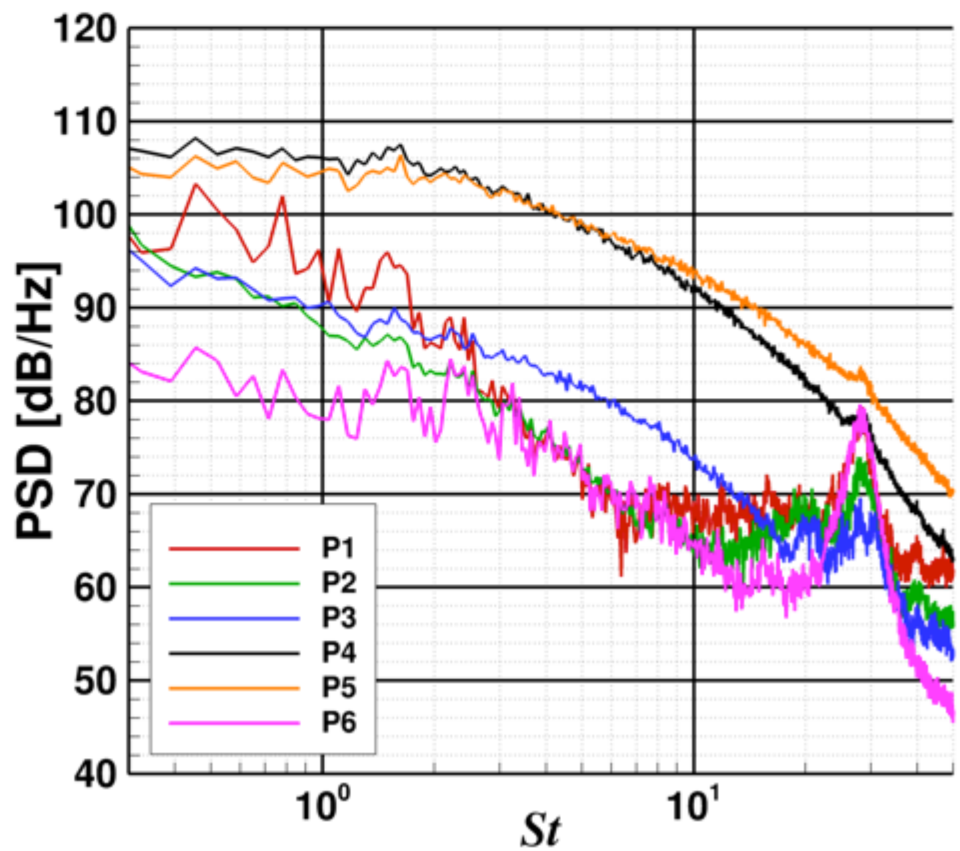

3rd AIAA BANC Workshop: Slat Cove Noise

Flow Field Visualizations

- Fine spanwise resolution in the slat cove is necessary to accurately resolve the turbulent kinetic energy in order to capture vortex sheet breakdown into 3D structures

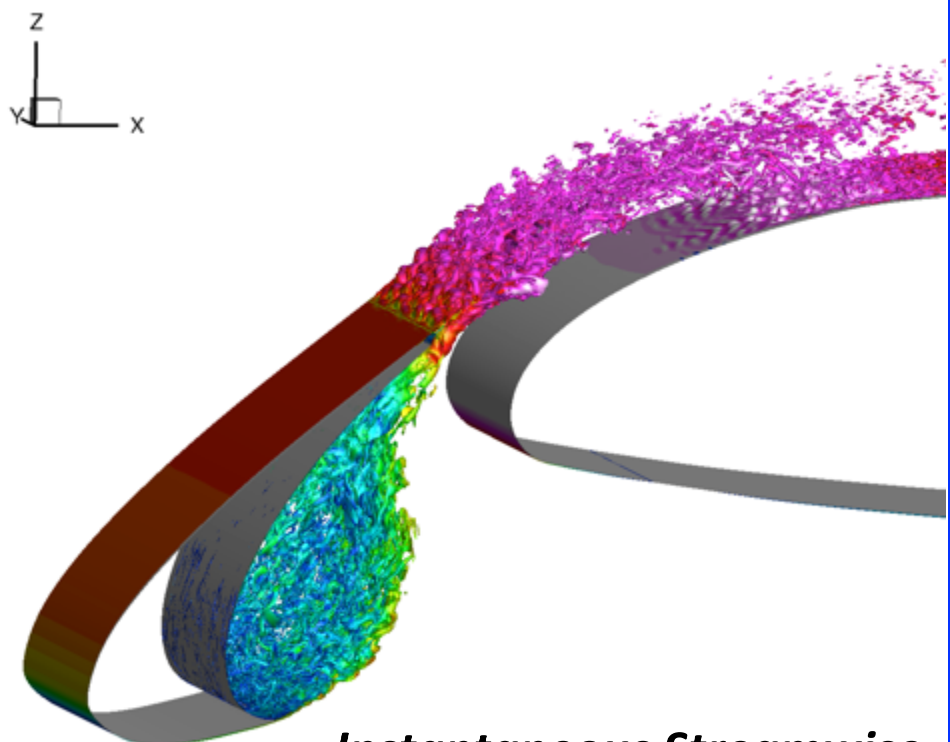

Instantaneous Streamwise Vorticity Isocontours

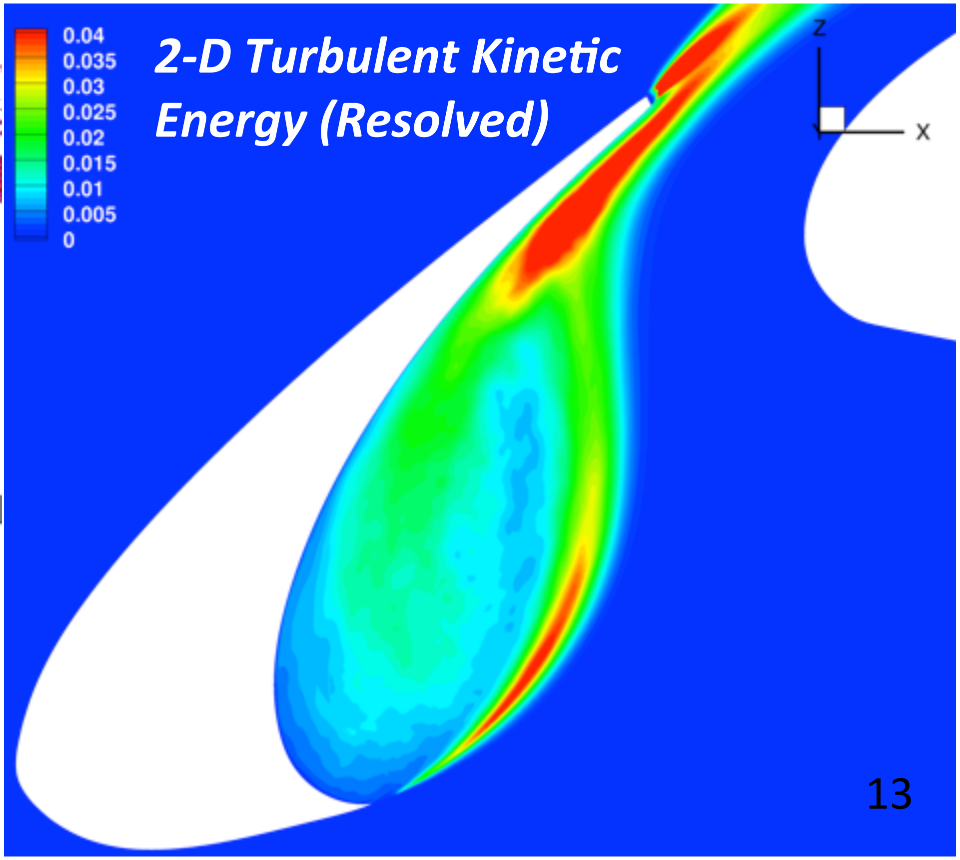

2-D Turbulent Kinetic Energy (Resolved)

Outline

- Objective and Approach
- Launch Ascent and Vehicle Aerodynamics (LAVA) Framework
- 3rd AIAA BANC Workshop
- **Aerodynamic Characterization of Slat Configuration**
- Summary

Aerodynamic Characterization of Slat Configuration

Procedure

- CFD validation of a conventional wing/slat model
- Steady-state deployment analysis of slat model in free-air
- Steady-state deployment analysis of slat model installed in QFF
- Comparison of free-air and installed deployment analysis
  - Angle of attack relation
  - Centerline Cp comparison
  - Centerline streamlines comparison

CFD Validation

Simplified QFF and Conventional Wing/Slat – Overset Grid System

- 28 zones and 45.5 M grid points
- Triple Fringe with No Orphans
- Wall y+ ≈ 1 over all viscous wall surfaces

Main Element Chord 16 inch

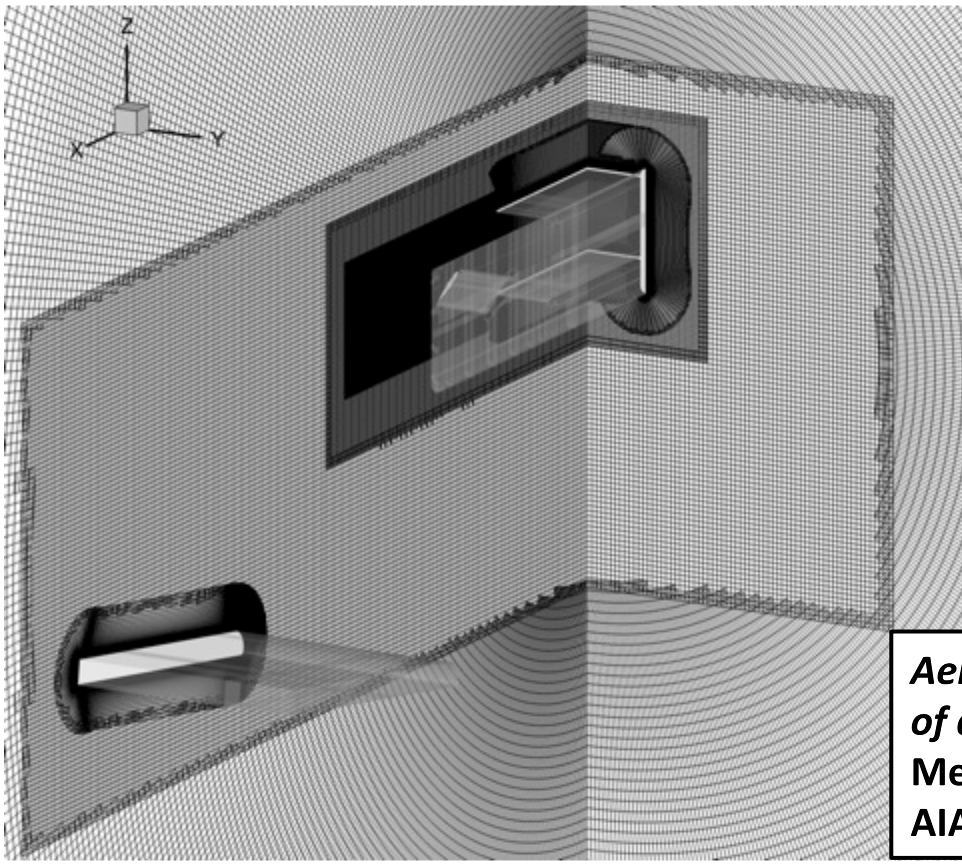

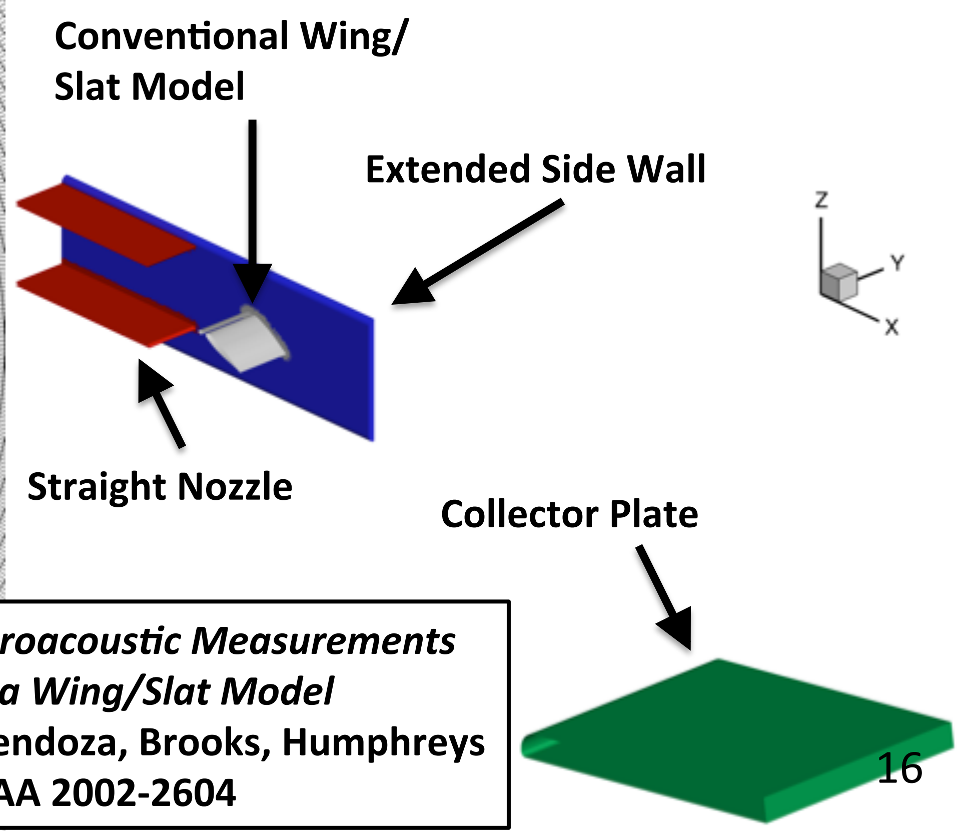

Aeroacoustic Measurements of a Wing/Slat Model
Mendoza, Brooks, Humphreys
AIAA 2002-2604

CFD Validation

U velocity contours on symmetry plane and at nozzle exit

- Initially isentropic flow relations were used to set the stagnation conditions at the nozzle plenum based on the desired nozzle exit jet velocity (neglecting viscous losses at the nozzle walls), which lead to a lower velocity than the experimental reference
- A sensitivity study was performed in which the stagnation pressure was varied and the exit velocity was monitored

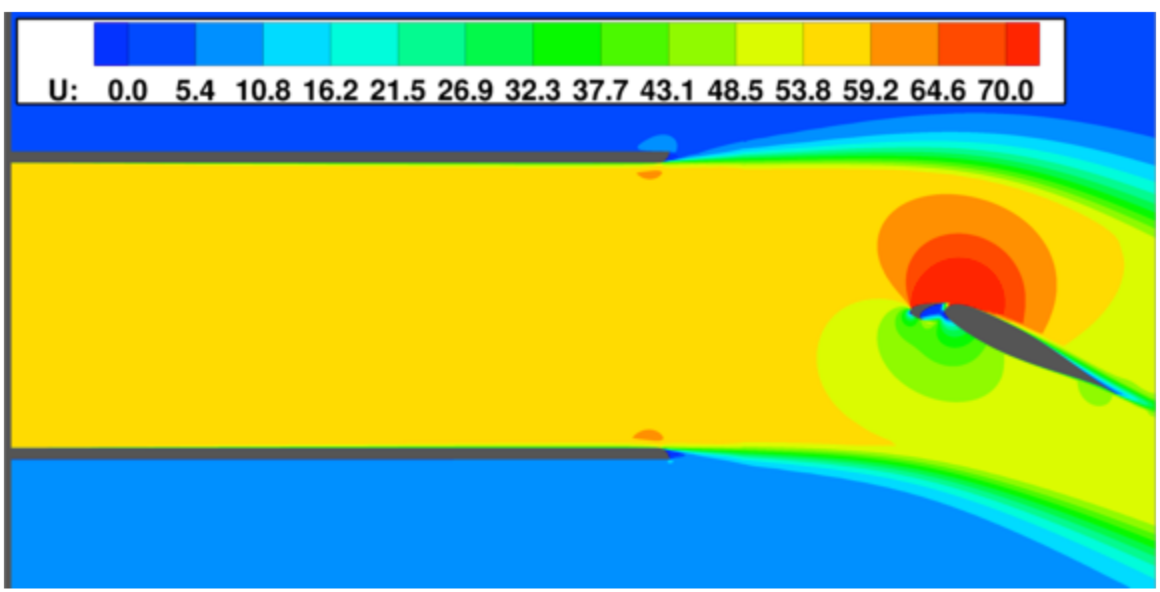

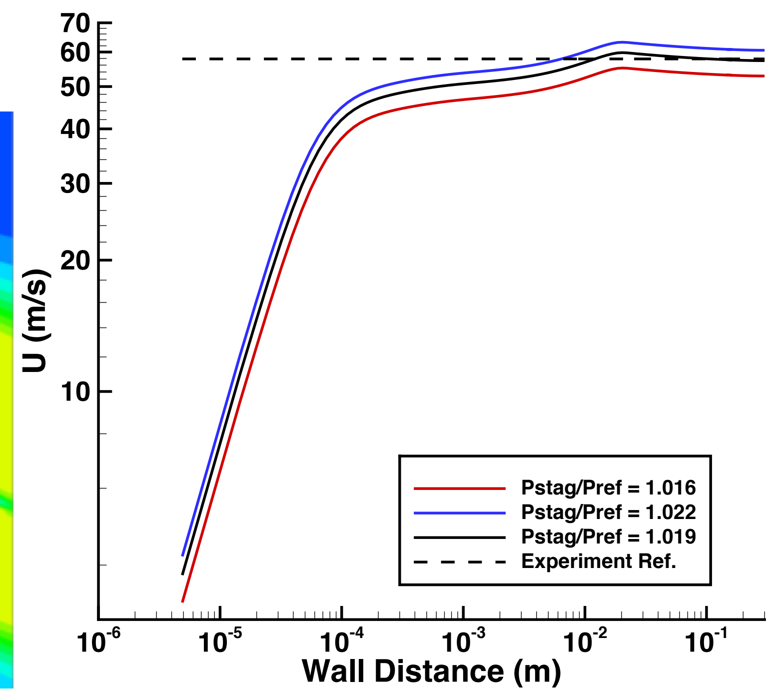

CFD Validation

Centerline Cp Comparison

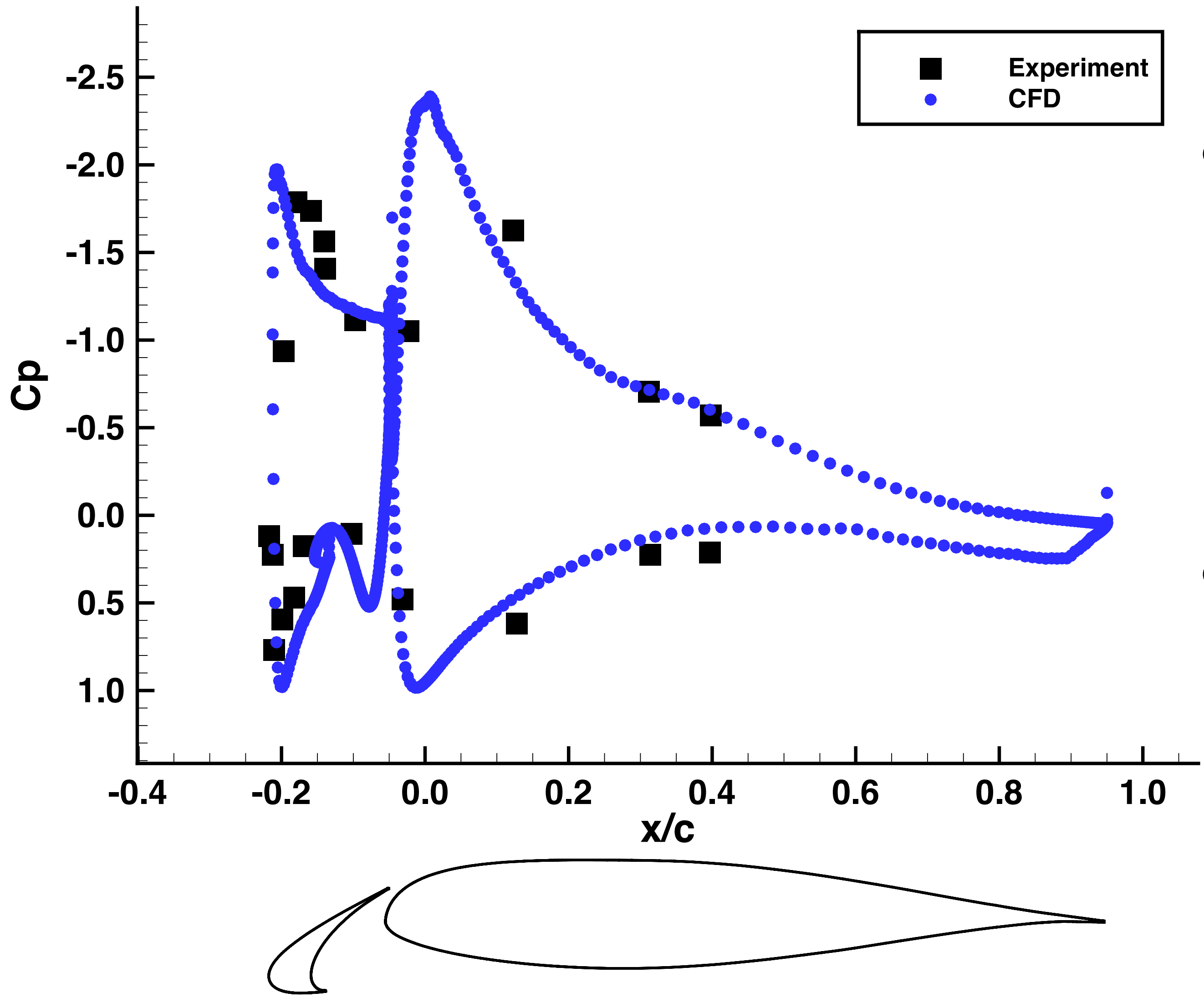

- Good match in centerline Cp is obtained
- Small differences on the pressure side of the main element and the suction side of the slat
- More accurate QFF geometry representations were analyzed, and overall comparison did not change

Free-Air Deployment Analysis

Conventional Slat Geometry

- **Modified 30P30N fully deployed in free-air**
- **Stowed-Flap C_{ME} = 16”**
- **Fully-Stowed C = 16.73”**
- **Nominally 2D (b = 0.8” CFD grid uses 5 planes in span)**

Deployment Parameter Space

- **A database of steady RANS analysis for free-air slat deployments has been performed (270 cases)**
  - **Notch 0, 4, 6, 8, and 9 (Gap/C_{ME} =0.032,0.025,0.021,0.018,0.016)**
  - **Slat Deployment Angle: 10º, 20º, 30º**
  - **Angle of Attack: 1.0º to 9.5º in 0.5º increments**

Free-Air Deployment Analysis

Lift Coefficient

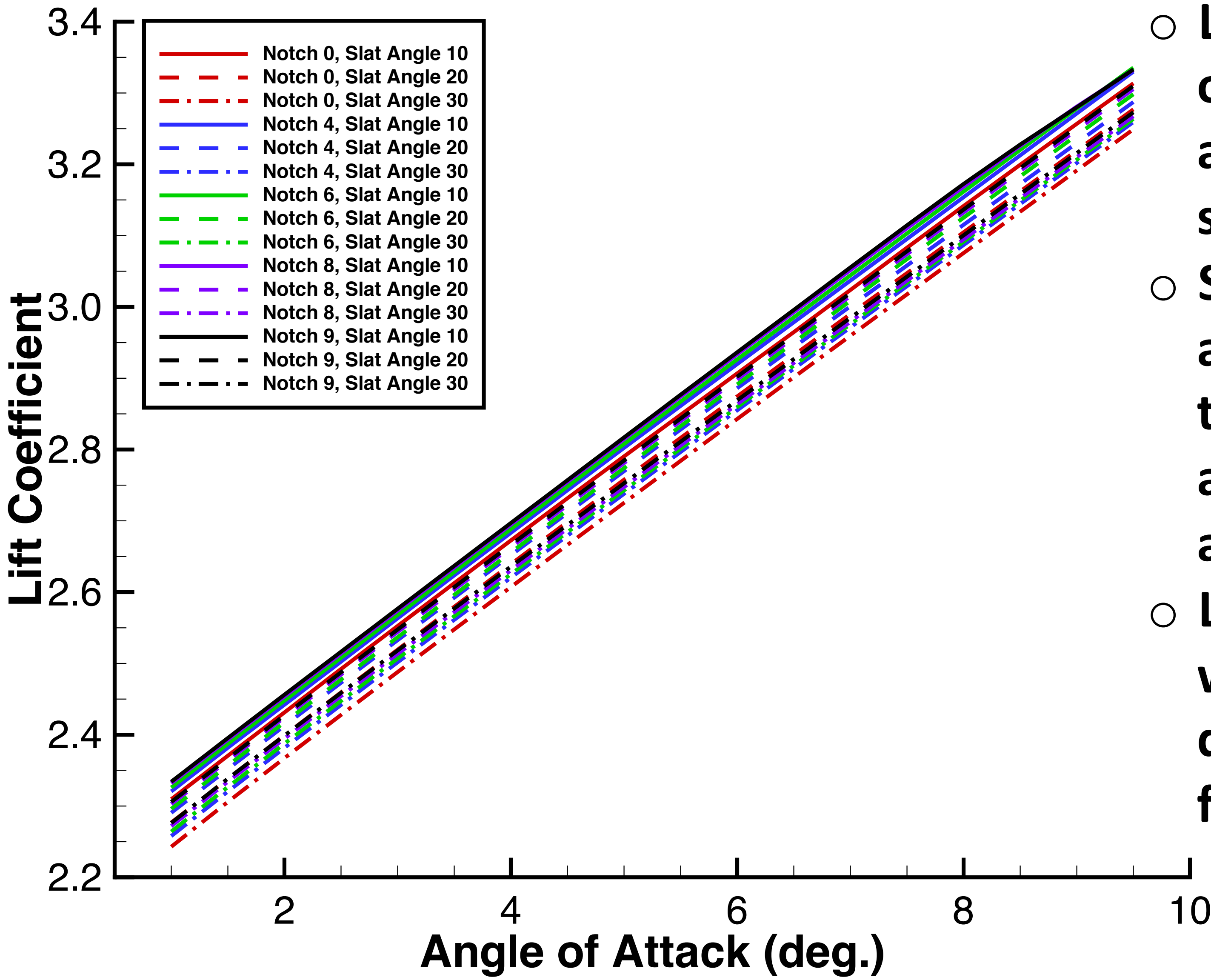

- **Linear behavior is observed over the angle of attack sweep**
- **Slat deployment angle 10 shows the largest lift for all gap distances and AOAs**
- **Lift decreases with increasing deployment angle for $1 \leq \alpha \leq 9.5$ deg.**

Free-Air Deployment Analysis

Lift Coefficient Component Breakdown: Notch 0

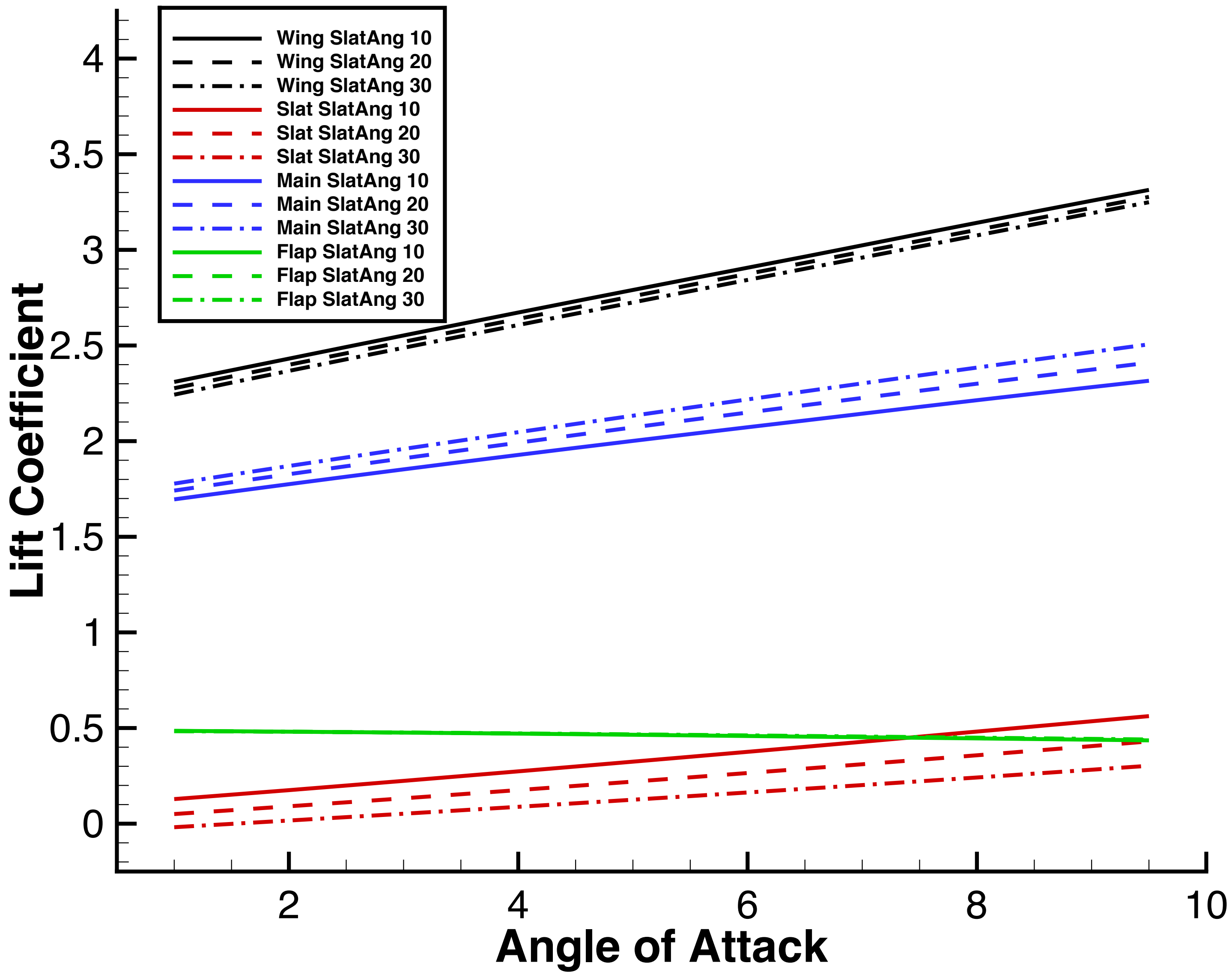

- The main element carries most of the lift and shows an increase in lift with increasing deployment angle
- Lift on the slat decreases with increasing deployment angle
- Lift on the flap is constant

Installed Deployment Analysis

Geometry and Slat Deployment Parameterization

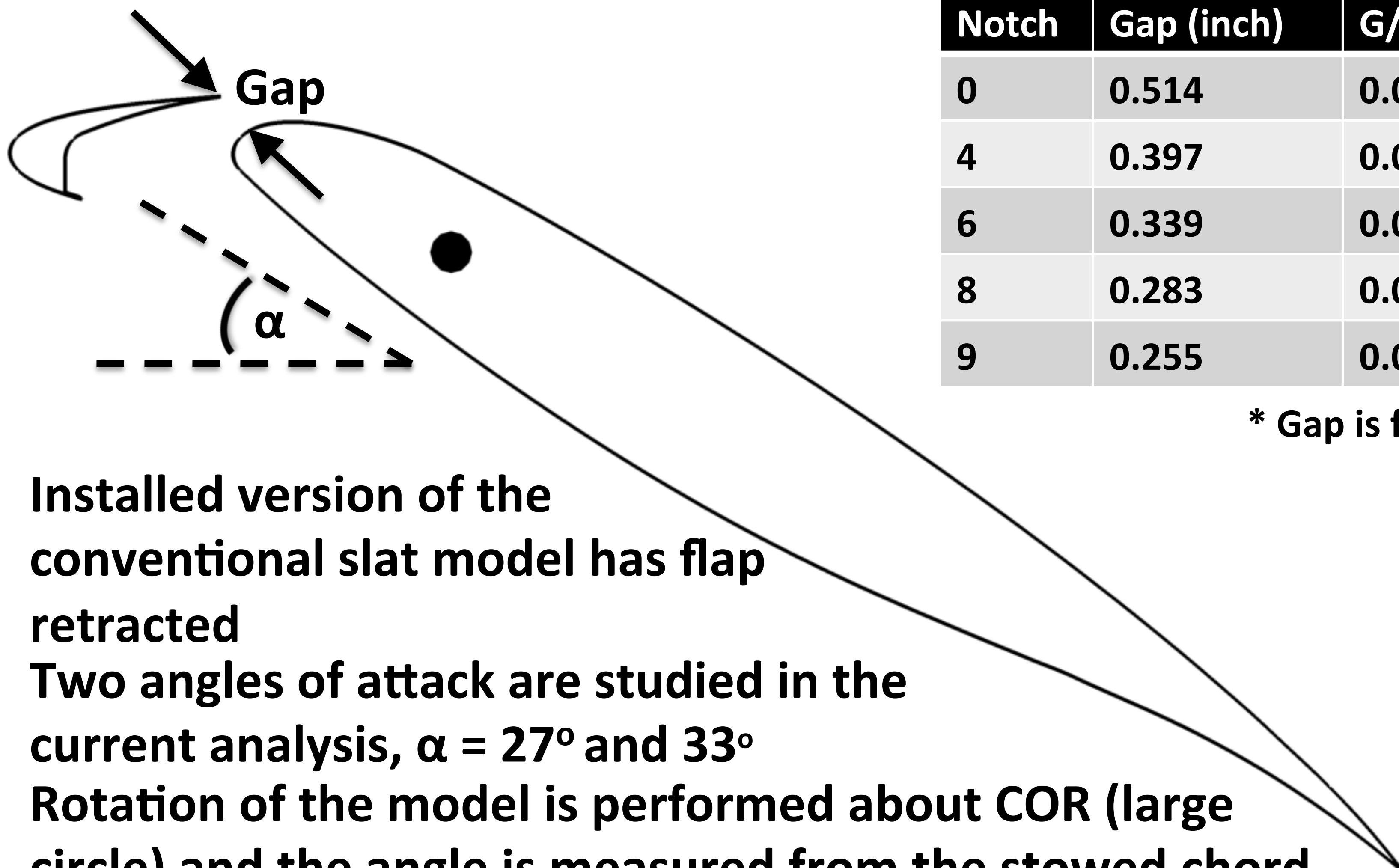

Notch	Gap (inch)	G/C_{ME}
0	0.514	0.032
4	0.397	0.025
6	0.339	0.021
8	0.283	0.018
9	0.255	0.016

* Gap is for $\alpha_s = 30^o$

- Installed version of the conventional slat model has flap retracted
- Two angles of attack are studied in the current analysis, $\alpha = 27^o$ and 33^o
- Rotation of the model is performed about COR (large circle) and the angle is measured from the stowed chord line

Installed Deployment Analysis

Structured Overset Grids

- **30 grid systems generated for each slat configuration and AOA with the slat and ME grids simply translated and rotated for each configuration**
- **40 zones and 109.6 M grid points for the full-span configuration with y+ ≈ 1 at all viscous walls**
- **A hemi-spherical off-body grid extends 400 chord lengths**

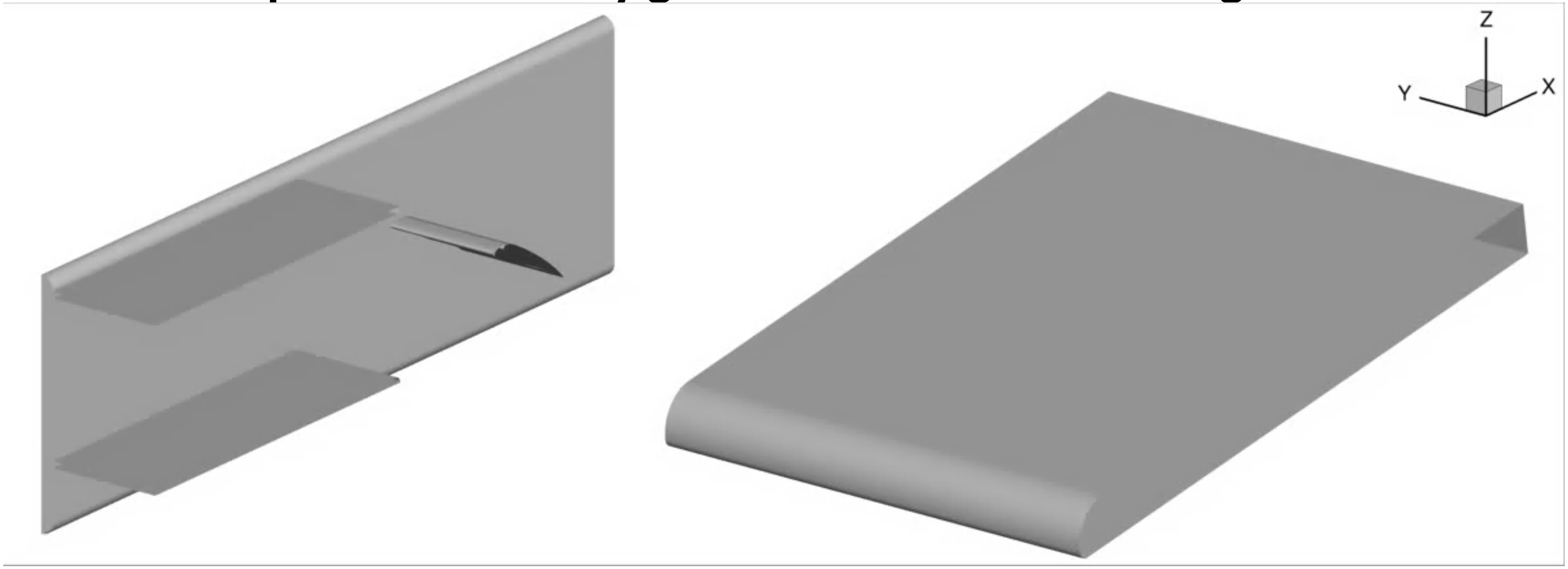

Installed Deployment Analysis

Centerline Cp Distributions: Notch 0 AOA 27°

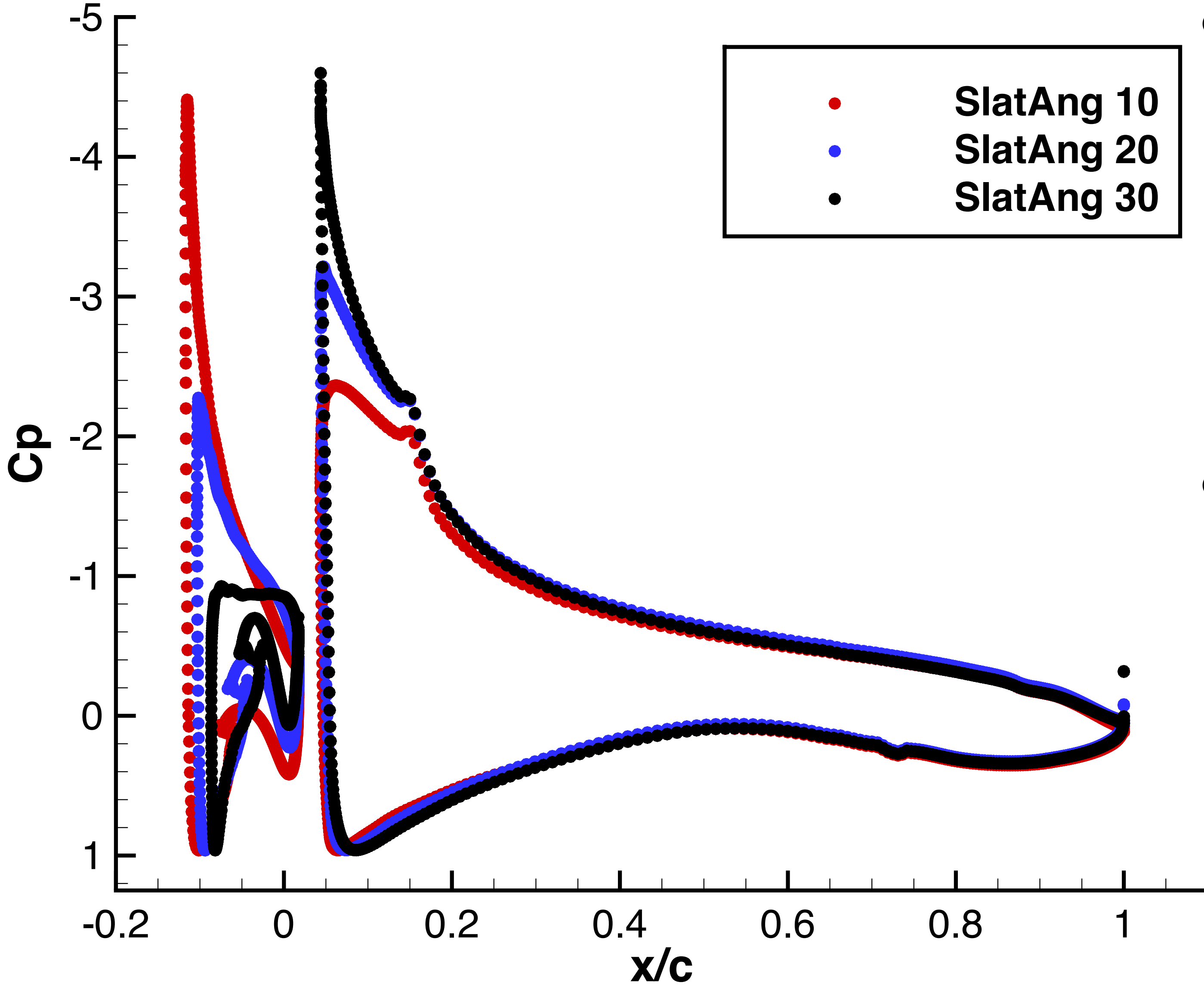

- Cp distribution on the slat decreases in magnitude with increasing deployment angle
- In contrast, the magnitude of the Cp increases on the main element with increasing deployment angle

Installed Deployment Analysis

Surface Streamlines AOA 27^o Notch 0

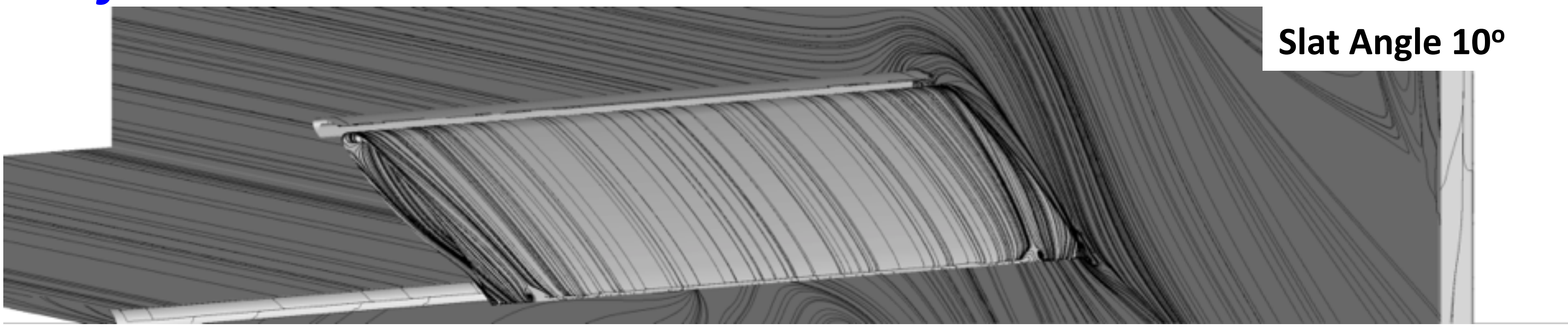

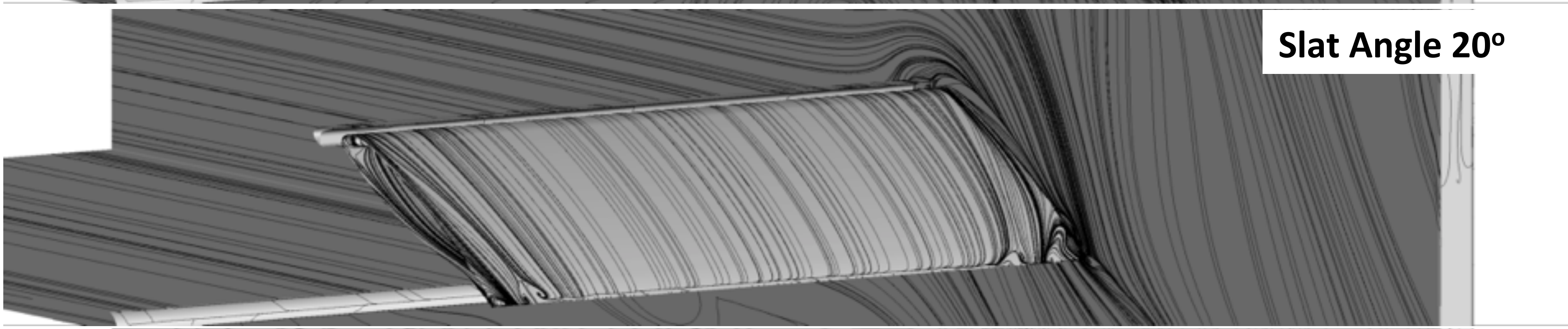

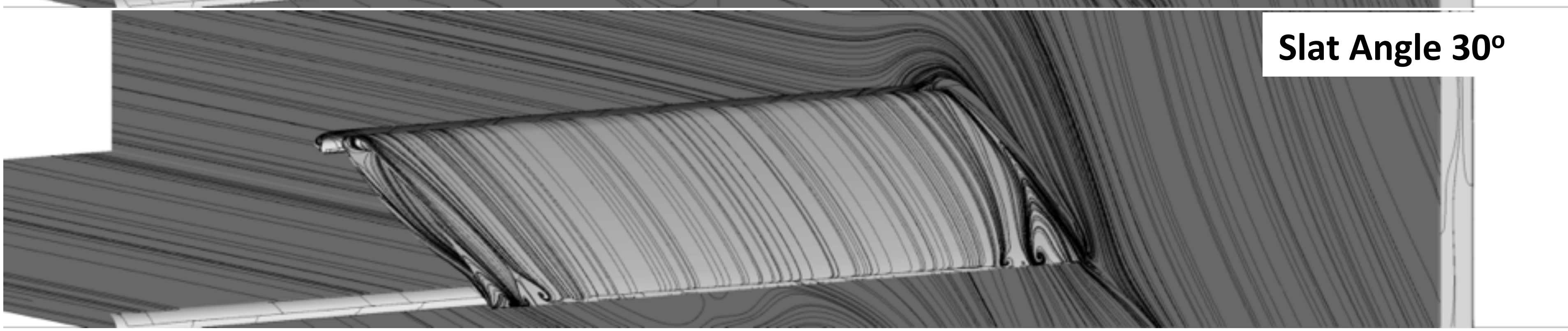

Installed Deployment Analysis

Surface Streamlines AOA 27° Notch 4

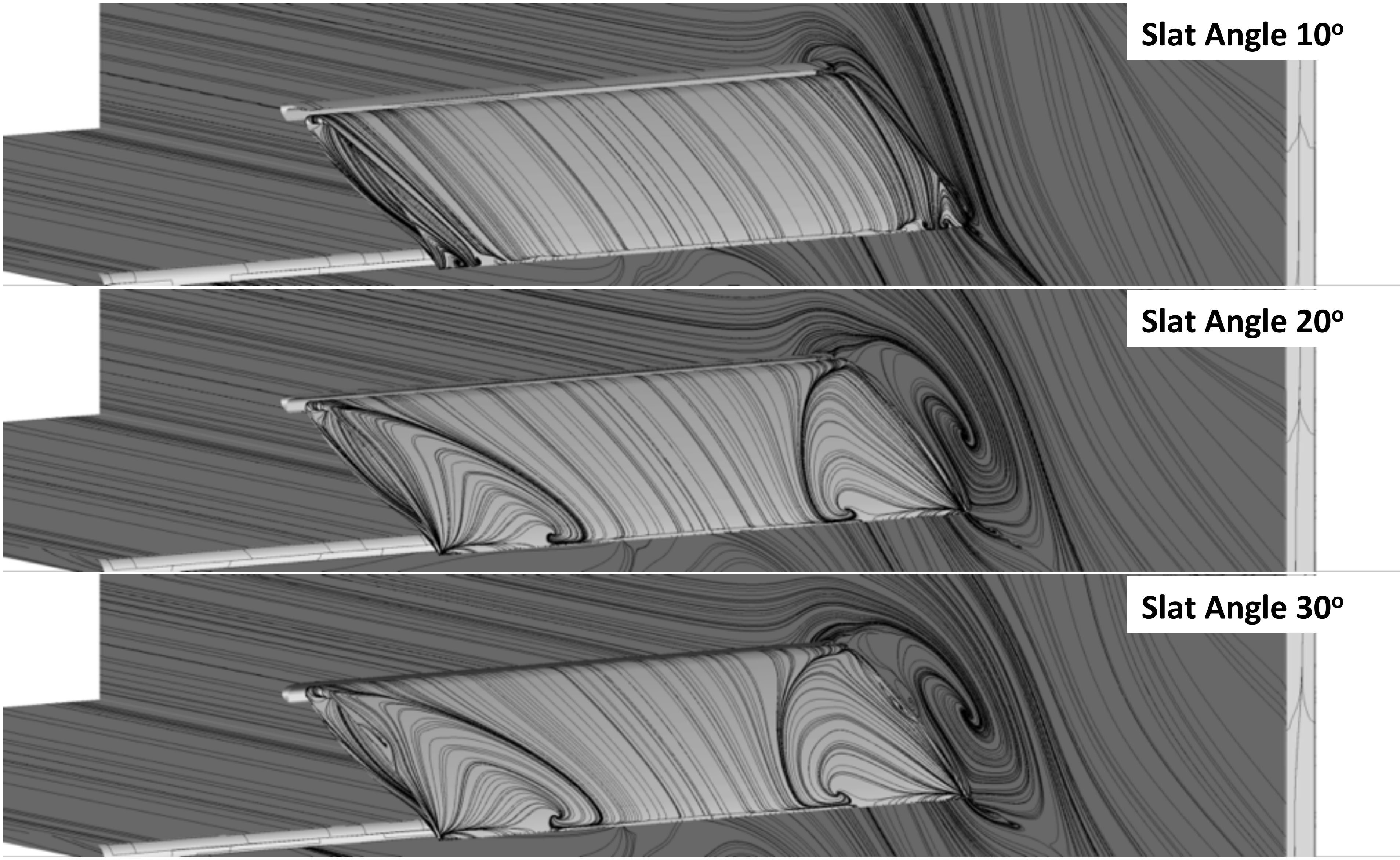

Free-Air/Installed Comparison

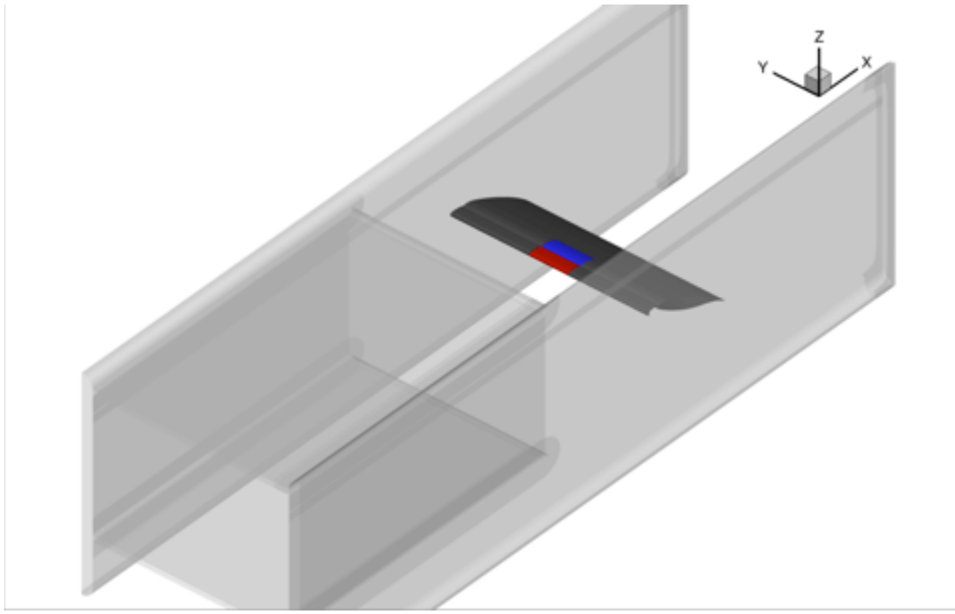

Force Integration Surface Definition for Comparison

- A subset of the slat and main element surfaces are used to compare the local aerodynamics of interest
- Main element $0 \leq x/c_{ME} \leq 0.2$
- Spanwise extent $-0.1 \leq y/b \leq 0.1$

WingSub

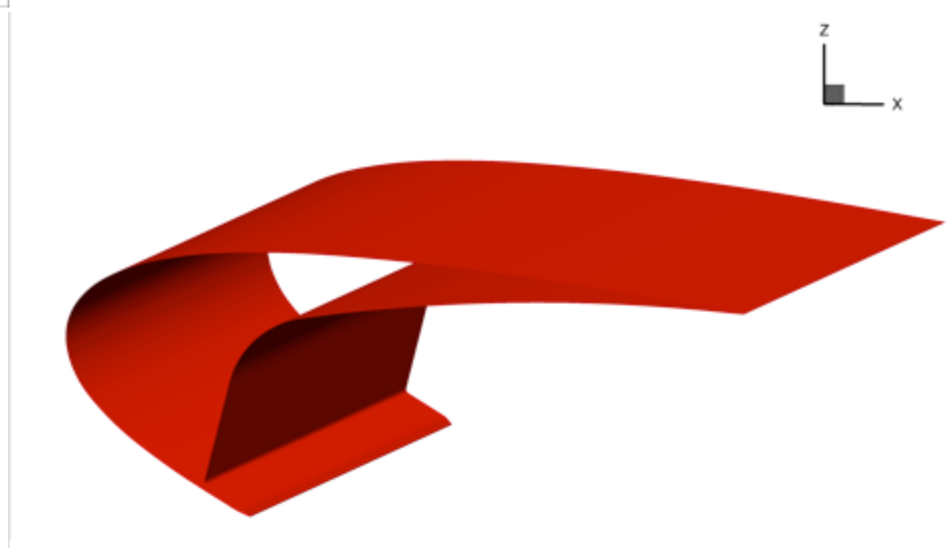

SlatSub

Free-Air/Installed Comparison

Free-Air/Installed WingSub AOA Comparison: Slat Angle 20°

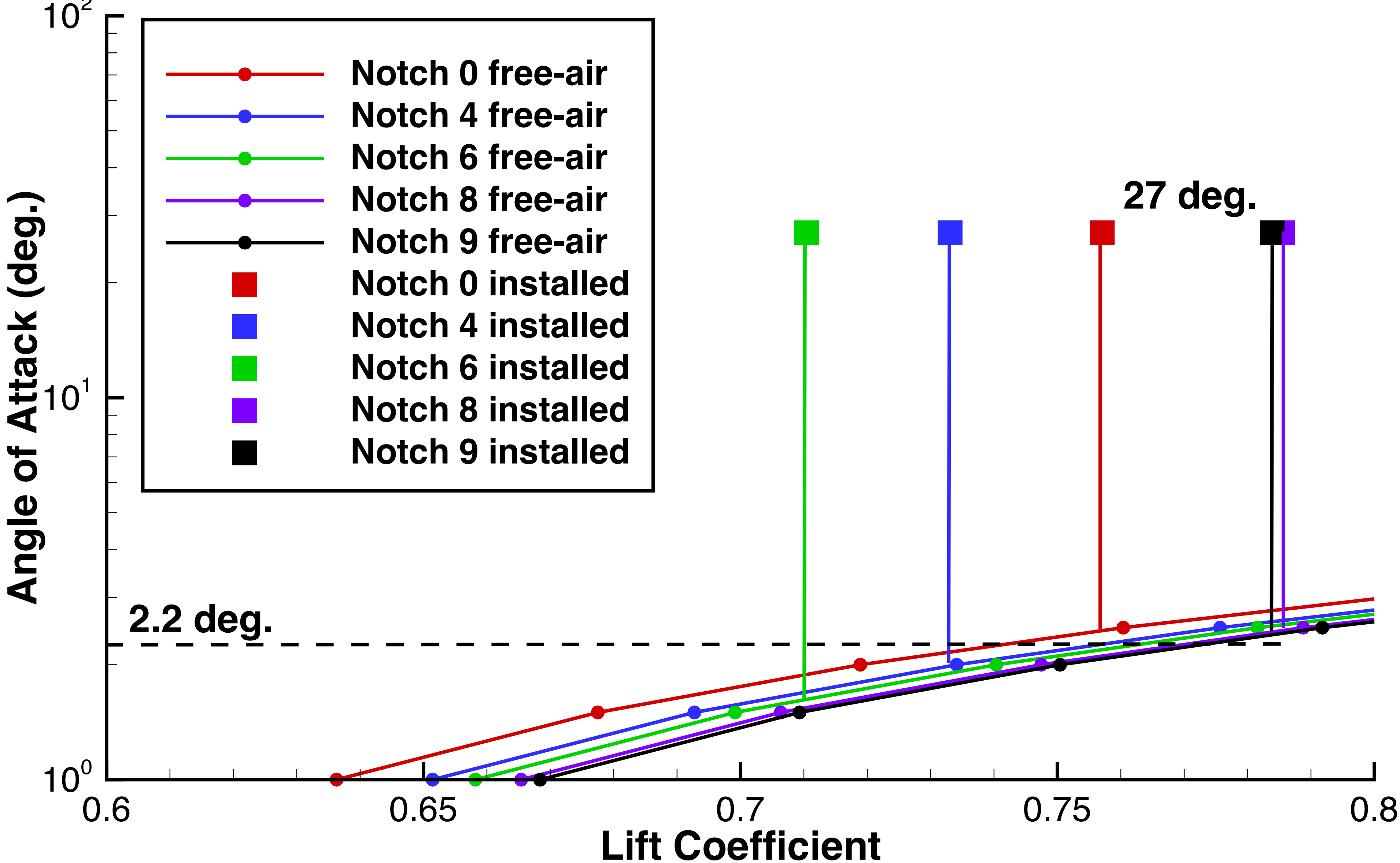

Free-Air/Installed Comparison

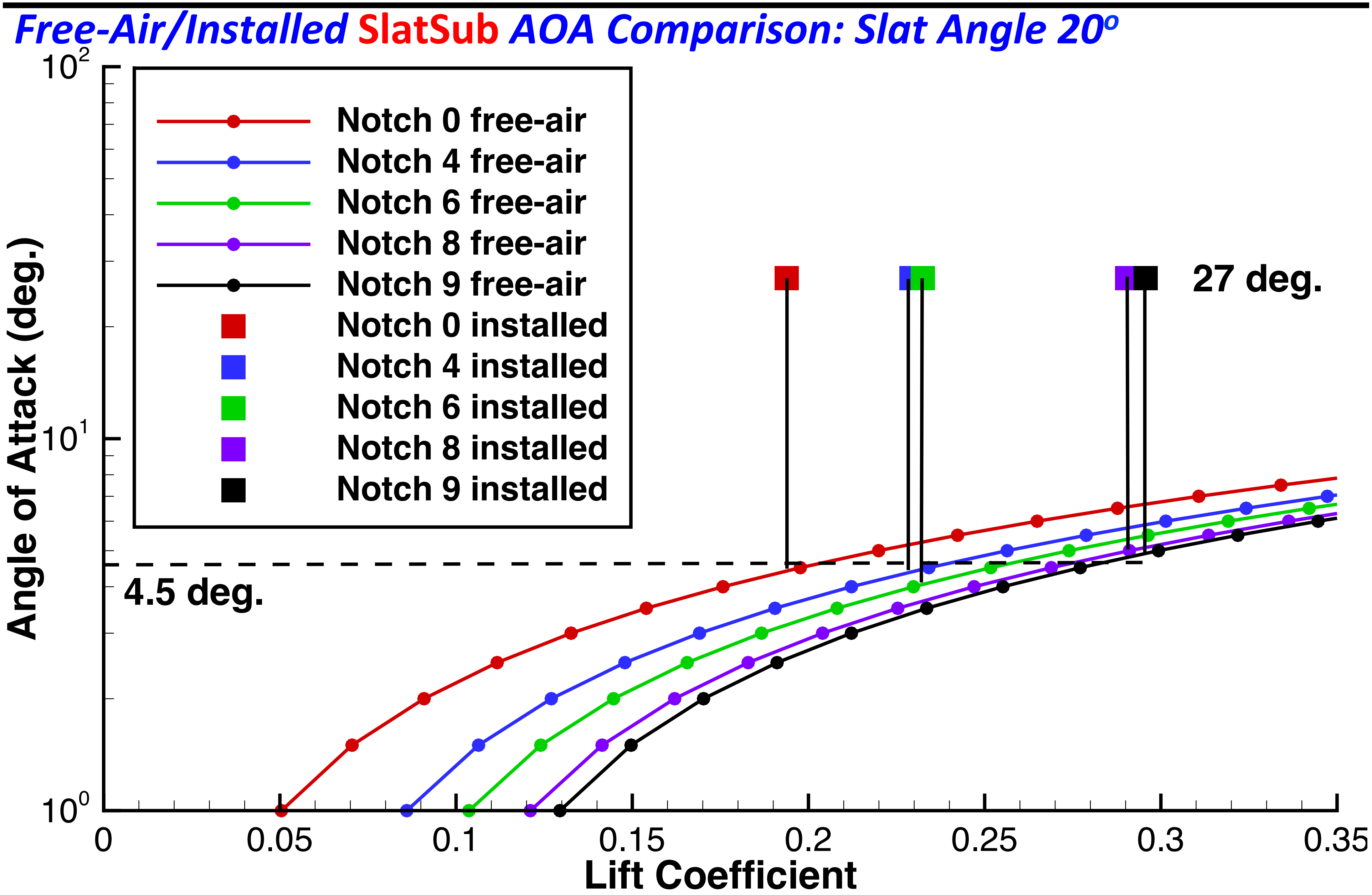

Free-Air/Installed Comparison

Cp Comparisons: Notch 0 Slat Angle 20°

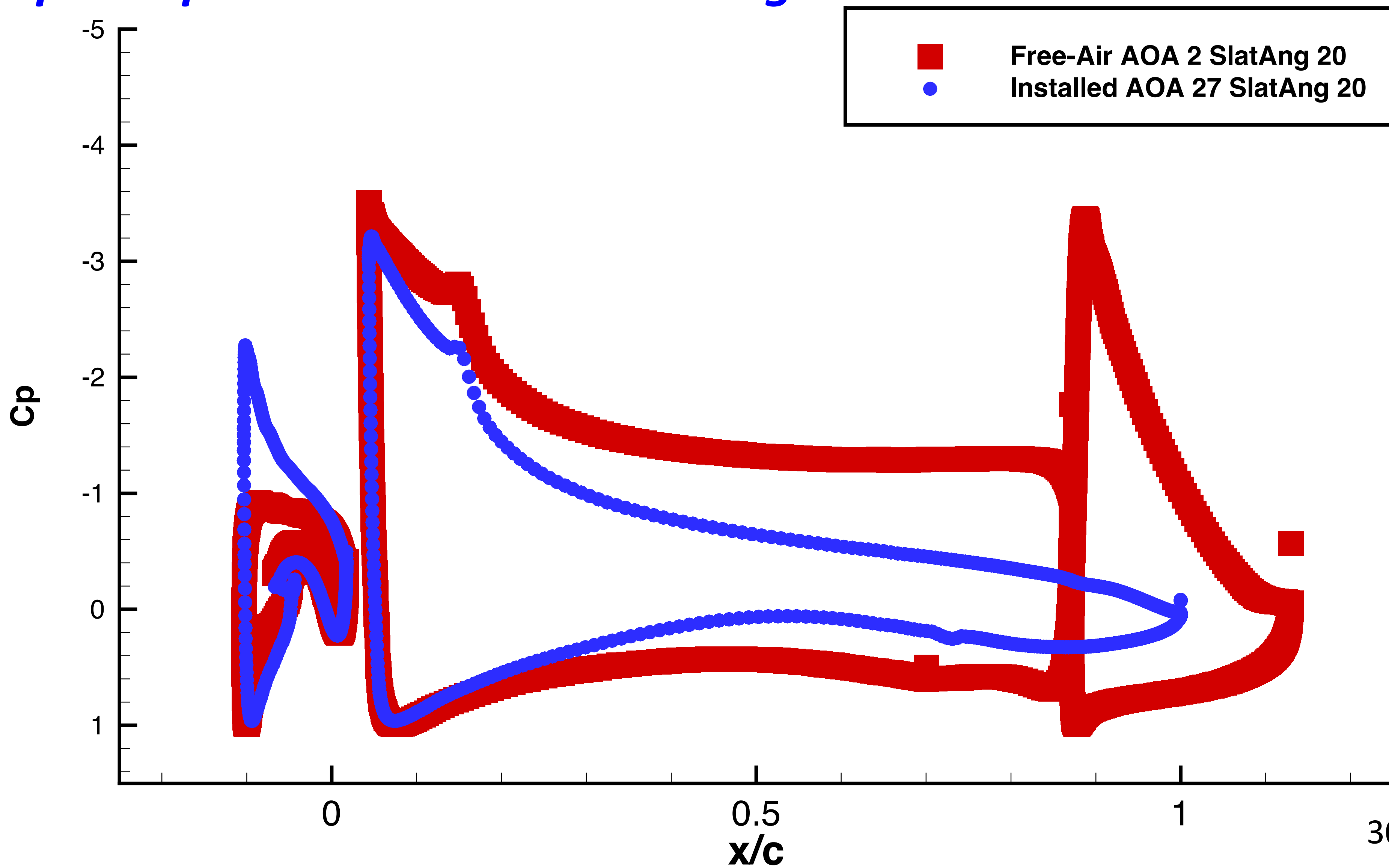

Free-Air/Installed Comparison

Cp Comparisons: Notch 0 Slat Angle 20° (and 30°)

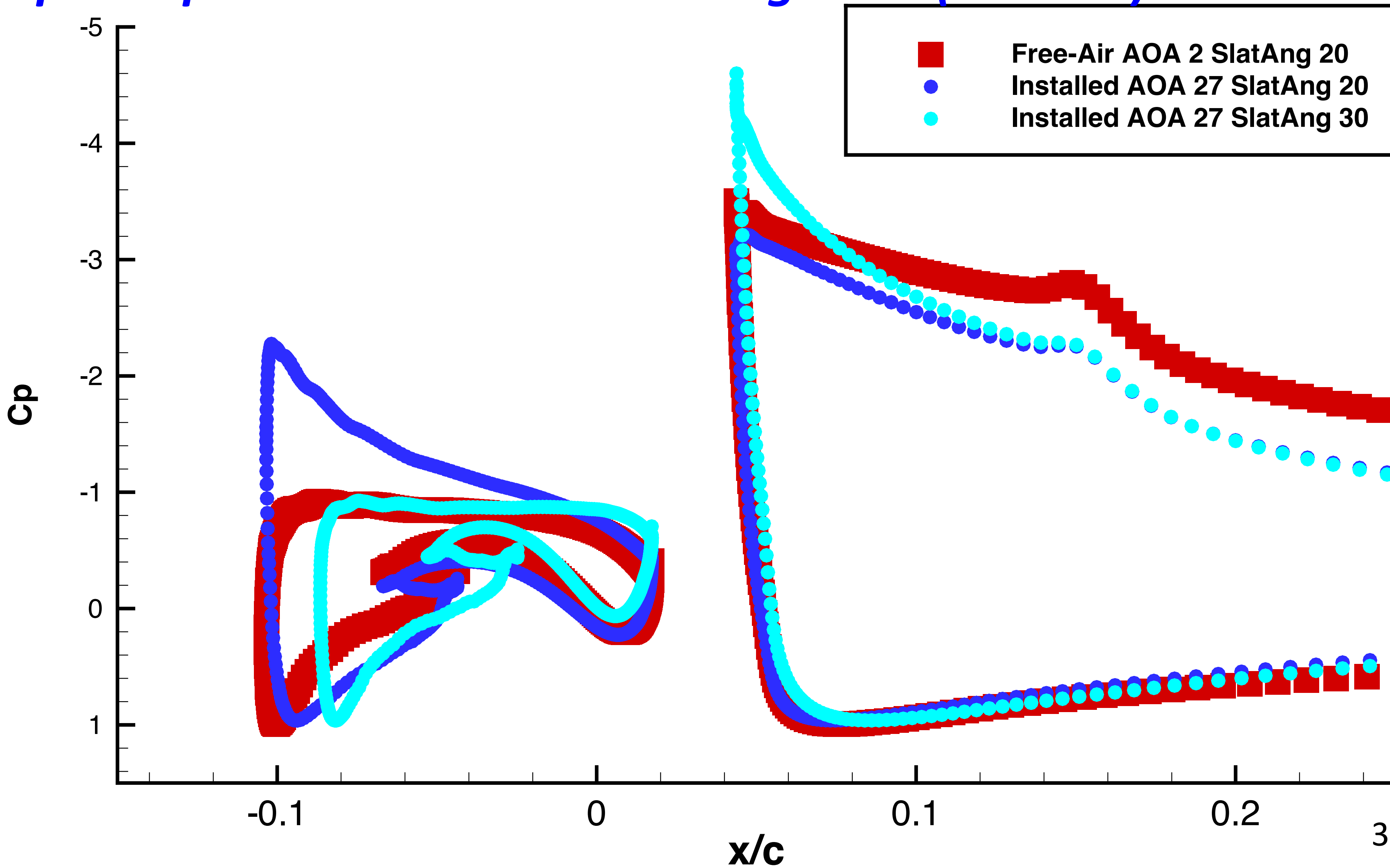

Free-Air/Installed Comparison

Cp Comparisons: Notch 0 Slat Angle 20°

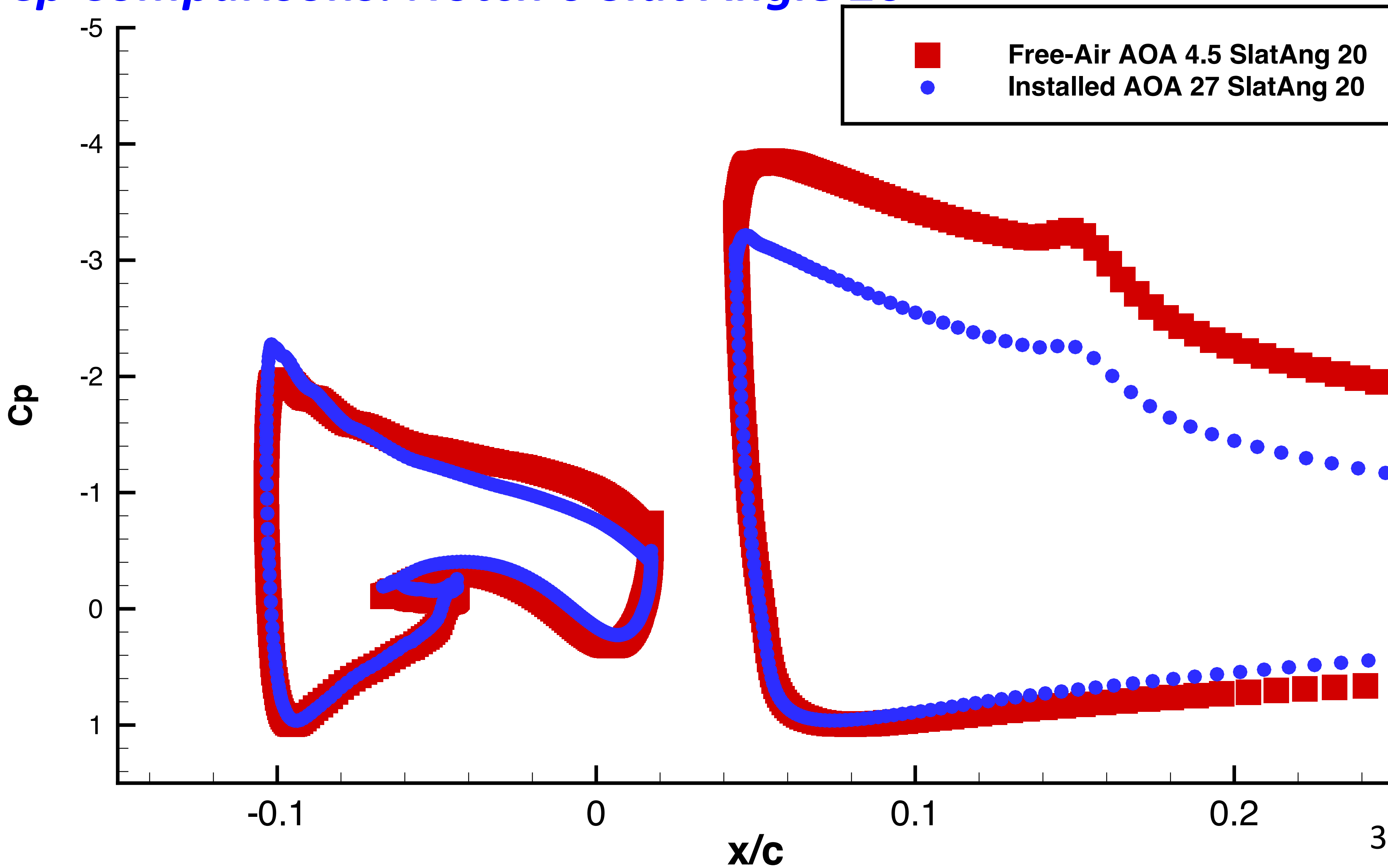

Free-Air/Installed Comparison

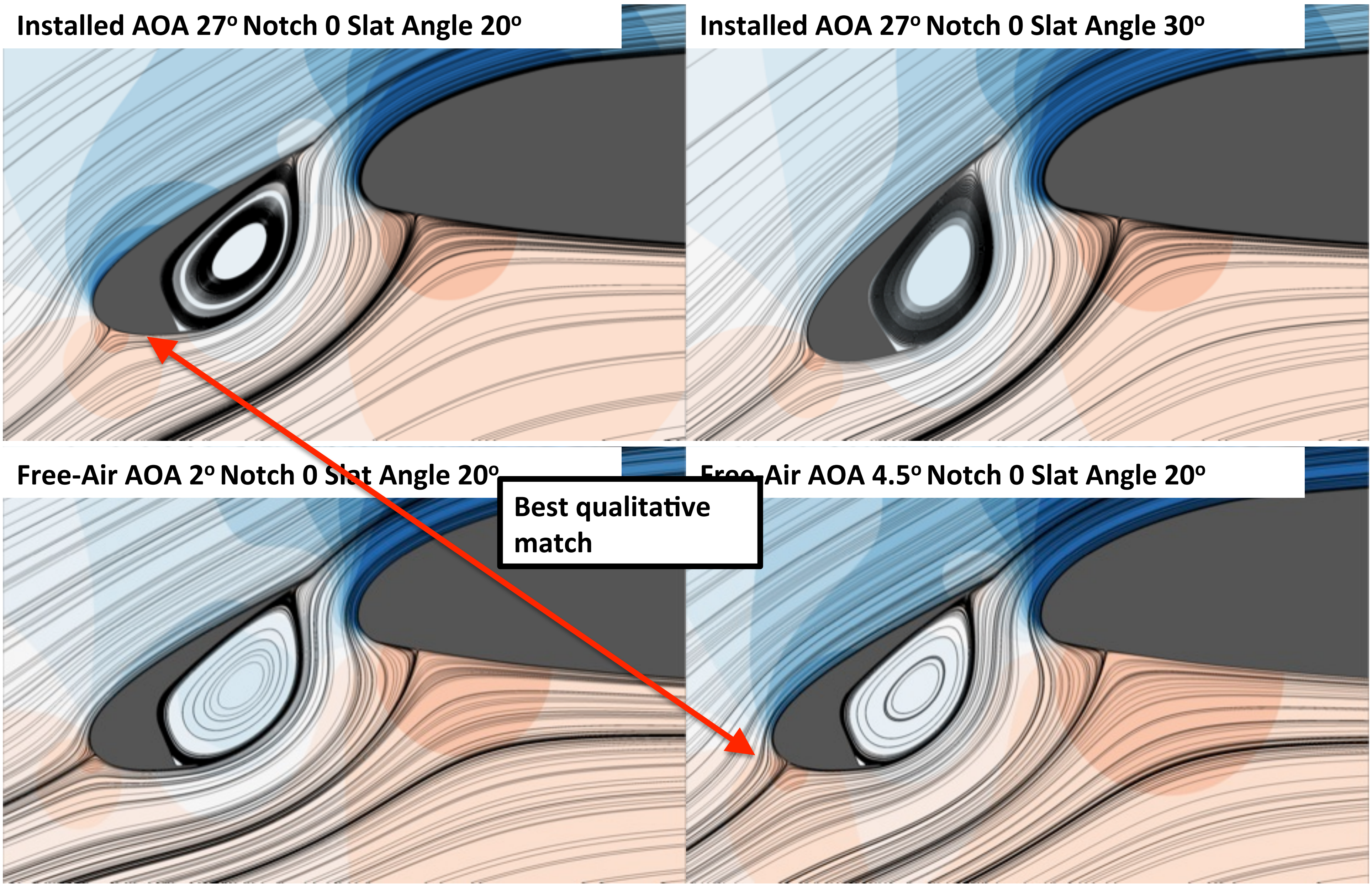

Summary

- The LAVA CFD/CAA analysis tools have been validated for this work using the BANC-III Workshop and data from AIAA-2002-2604
- A free-air slat deployment study was performed on the modified 30P30N model showing a linear increase in lift with AOA
- A component breakdown of lift indicates the main element carries most of the lift, increasing with deployment angle, but the lift on the slat decreases faster with increased deployment
- A QFF installed deployment study was performed on the conventional slat with the flap retracted showing side-wall induced separation on the main element with decreasing gap distance and increasing deployment angle
- Two integration surface subset were used to derive a free-air/installed angle of attack relation for the local aerodynamics
- Comparing the centerline Cp and streamline patterns, based on the angle of attack relations, indicates that matching the lift on the slat leads to a reasonably good match in local aerodynamics

Acknowledgements

- Russell Thomas and Casey Burley from NASA Langley Research Center
- NASA Advanced Supercomputing (NAS) Center